Photocurrent-Assisted Wavelength (PAW) Conversion With Electrical Monitoring Capability Using a Traveling-Wave Electroabsorption Modulator

Hsu-Feng Chou, Yi-Jen Chiu, Adrian Keating, John E. Bowers, *Fellow, IEEE*, and Daniel J. Blumenthal, *Fellow, IEEE*

***Abstract*—A new mechanism of cross-absorption modulation is proposed and experimentally demonstrated to assist wavelength conversion using a traveling-wave electroabsorption modulator (TW-EAM). The photocurrent signal generated by the pump propagates along the TW electrodes and changes the absorption of the waveguide, which imprints data to the probe. The photocurrent signal can also be received by an external electronic circuit to provide monitoring capability. This photocurrent-assisted mechanism does not rely on the saturation of absorption and has the potential to reduce the high pumping power required by EAM-based wavelength converters. Using 2.5-Gb/s nonreturn-to-zero data, the conversion range can cover 30 nm in C-band and the lowest power penalty is 0.5 dB.**

***Index Terms*—Cross-absorption modulation, electroabsorption, traveling-wave (TW) device, wavelength conversion, wavelength-division multiplexing.**

I. Introduction

WAVELENGTH converters will be key elements to enable wavelength routing and resolve wavelength contention in advanced photonic networks. Electroabsorption modulators (EAMs) have been demonstrated as compact wavelength converters [1] and optical regenerators [2]–[4] by utilizing either cross-absorption modulation (XAM) or cross-phase modulation (XPM). While high-speed conversion up to 80 Gb/s has been reported using XPM with a delayed interferometer [1], those using XAM have simpler configurations and can be a preferred choice at lower bit rates. However, one of the main problems is the high pumping power required, typically 16$\sim$19 dBm, as it is inefficient and affects long term reliability [5].

Conventionally, XAM in EAMs is attributed to the field-screening effect, caused by a large number of photogenerated carriers [2]. The screening of the external field lowers the absorption of a reverse-biased EAM and opens a transmission window for the probe. To obtain a decent extinction ratio, a high pumping power is necessary to excite sufficient carriers. However, we propose that, in a traveling-wave EAM (TW-EAM), there is another XAM mechanism which does not rely on the saturation of absorption. This mechanism utilizes the photocurrent signal generated by the pump to modulate the absorption of the EAM as the signal propagates along the TW electrodes. Furthermore, after propagating out of the TW-EAM, the photocurrent signal can subsequently be received to provide electrical monitoring. We demonstrate these concepts using wavelength conversion with 2.5-Gb/s nonreturn-to-zero (NRZ) data format.

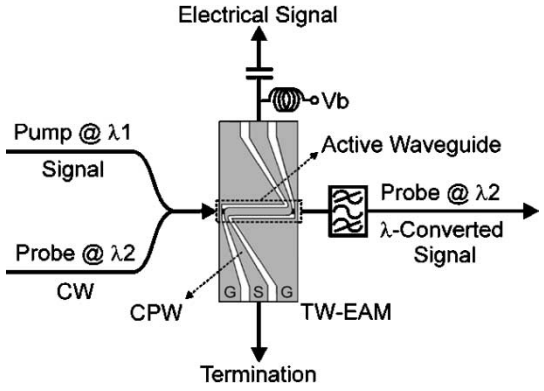

Fig. 1. Configuration of PAW-Conversion using a TW-EAM.

II. Principle of PAW-Conversion

TW-EAMs are designed with TW electrodes to overcome the *RC*-time limitation [6]. Therefore, the active device length can be much longer than a lumped-element EAM with the same bandwidth. The active waveguide and the feed electrodes are 300 and 500 μm long, respectively, for the TW-EAM used in this work [7]. The maximum modulation efficiency varies from 15 to 30 dB/V in C-band, depending on the polarization and bias voltage.

The configuration of the photocurrent-assisted wavelength conversion (PAW-Conversion) using a TW-EAM is shown schematically in Fig. 1. Co-propagation of the pump and the probe is assumed, which is a preferred configuration for TW-EAM at high speed [8]. When the pump enters the reverse-biased TW-EAM, it gets absorbed and generates electron-hole pairs in the active region. These carriers are swept to the electrodes by the external field (due to reverse bias) and excite microwave propagation modes of the coplanar waveguide (CPW), just like a high-speed photodetector. The higher the external field (reverse bias), the shorter the sweep-out time. The excited microwave signal, which will be called "photocurrent signal" in the rest of the paper, propagates in

Manuscript received June 24, 2003; revised September 11, 2003. This work was funded by DARPA/MTO under CS-WDM Grant N66001-02-C-8026.

H.-F. Chou, A. Keating, J. E. Bowers, and D. J. Blumenthal are with the Department of Electrical and Computer Engineering, University of California, Santa Barbara, CA 93106-9560 USA (e-mail: hubert@ece.ucsb.edu).

Y.-J. Chiu was with the Department of Electrical and Computer Engineering, University of California, Santa Barbara, CA 93106-9560 USA. He is now with the Institute of Electro-Optical Engineering, National Sun Yat-sen University, Kaohsiung 80441, Taiwan, R.O.C.

Digital Object Identifier 10.1109/LPT.2003.821095

both directions along the TW electrodes. Since the TW-EAM is highly absorptive under reverse bias, most of the pump is absorbed near the input facet of the active waveguide. Half of the photocurrent signal propagates to the left and finally goes to the termination. The other half of photocurrent signal propagates to the right, heading toward the upper end of the CPW line. When the photocurrent signal is passing through the active waveguide, it modulates the local voltage around the dc bias and, as a result, changes the absorption experienced by the probe. Therefore, the signal carried by the pump is first transferred to photocurrent through photodetection and then to the probe through electroabsorption, all in the same waveguide. Since photocurrent plays an intermediate role in this process, this mechanism is called photocurrent assisted. The photocurrent signal can subsequently be received by outside electronics to provide signal monitoring, which adds an extra functionality to PAW-Conversion and increases overall power utilization.

In the saturation mechanism, a large number of carriers must be generated to produce sufficient field screening to get a high extinction ratio. This imposes a requirement for high pumping power. On the other hand, these carriers must be swept out of the active region as fast as possible to ensure high-speed operation. Unfortunately, the sweep-out time increases with the number of carriers [9], and EAM-based wavelength converters using the saturation mechanism have an inherent tradeoff between speed and extinction ratio. However, in the photocurrent-assisted mechanism, absorption saturation due to field screening is not required. Therefore, the pumping power can be reduced. Although the extinction ratio still depends on the pumping power, which determines the strength of photocurrent signal, it can be compensated by other factors such as the length of active waveguide and the value of microwave impedance.

PAW-Conversion is conceptually close to O-E-O optoelectronic wavelength converters [10] but in a more compact and integrated form. In PAW-Conversion, the conversion happens in the same waveguide, which reduces problems such as microwave loss and impedance mismatch in O-E-O converters. Also, it does not require two kinds of active region for the photodetector and the modulator.

III. Experimental Results and Discussion

Wavelength conversion of 2.5-Gb/s NRZ data is demonstrated. The pump is 13 dBm at 1545.8 nm with transverse magnetic (TM) polarization and the probe is 1 dBm CW at 1555.2 nm with transverse electric (TE) polarization. TM polarization generates more photocurrent and TE polarization has less loss. The current polarization dependence can be reduced by compensating the strain in the quantum wells [6]. The fiber-to-fiber transmission is shown in Fig. 1 of [8]. The reverse bias voltage is 0.8 V. A 2.4–nm optical bandpass filter is used to block the pump after wavelength conversion. Referring to Fig. 1, the upper end of the CPW line is connected to a bias-T and a sampling scope, which detects the photocurrent signal and also provides a 50-Ω termination. To verify the existence of photocurrent-assisted mechanism, two kinds of termination are used at the lower end of the CPW line. One is 50 Ω and the other is open. The photocurrent signal will

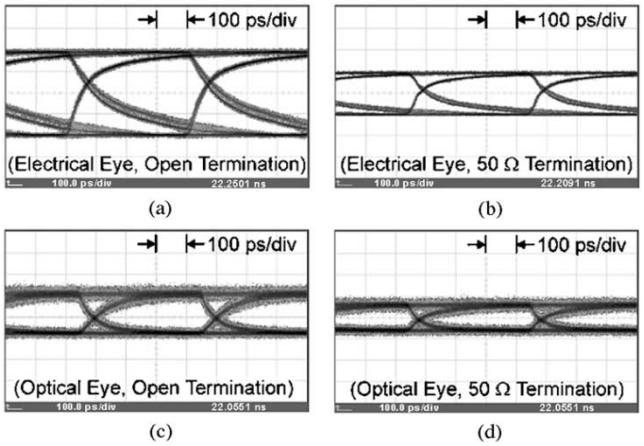

Fig. 2. Eye histograms of photocurrent signal (electrical) and wavelength converted signal (optical). The electrical eyes are taken with 6-dB attenuation. (a) Electrical eye with open termination. (b) Electrical eye with 50-Ω termination. (c) Optical eye with open termination. (d) Optical eye with 50-Ω termination.

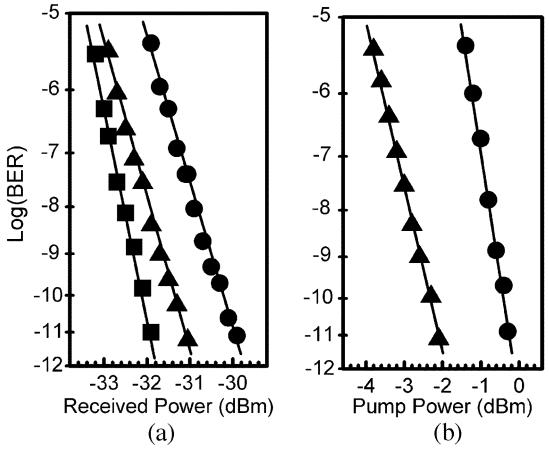

Fig. 3. BER curves of (a) optical signals and (b) electrical signals. Square: optical back-to-back at 1545.8 nm. Triangle: open termination. Circle: 50-Ω termination.

be terminated without reflection by 50-Ω termination. On the other hand, an open termination will reflect the photocurrent signal back to the active waveguide. If wavelength conversion is realized only by the saturation mechanism, there should be no difference between the two configurations. Fig. 2 shows the eye histograms of the photocurrent signal (electrical) and the wavelength converted signal (optical). The electrical eye amplitude for 50-Ω termination is 417 mV_{pp} and 829 mV_{pp} for open termination, which is almost doubled because of the reflection. The optical eye for open termination is also larger in amplitude, which indicates that the photocurrent-assisted mechanism does influence the wavelength conversion. Bit-error-rate (BER) curves are shown in Fig. 3(a). The optical power penalty for open termination is 0.5 and 1.5 dB for 50-Ω termination, which is a result of the difference in optical eye amplitude. The photocurrent signal is fed into the BER tester to measure the BER. At 13 dBm of pump power, no error was detected with both terminations. Therefore, the pump power is lowered to measure the BER. The results are shown in Fig. 3(b). The sensitivity at 10^{-9} BER is about 2 dB lower

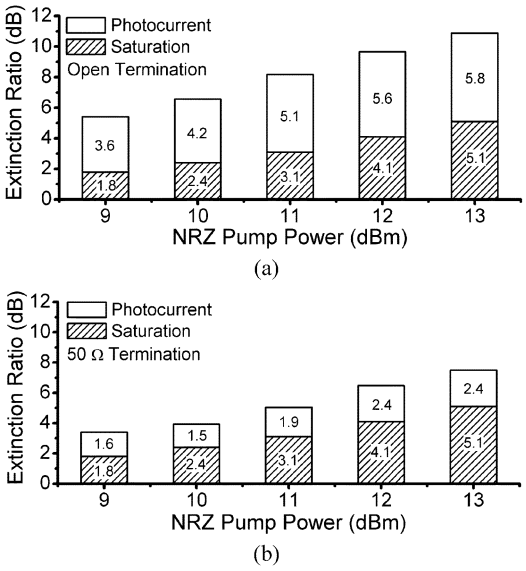

Fig. 4. Contribution of extinction ratio from different mechanisms as a function of NRZ pump power (a) with open termination and (b) with 50-Ω termination.

for open termination, mainly due to its larger electrical eye amplitude. The slight decrease in slope may be caused by the reflection from the open termination, which increases jitter and multiple reflections. The CPW line leading to the open termination can be cut shorter to minimize the round-trip time to the termination.

At high pumping powers, the saturation mechanism may also exist. To identify the contribution from this mechanism, the pump is changed from NRZ data to CW with twice the average power. In terms of power level, this CW pump can simulate the "1" bits when it is turned on, and when it is turned off, it simulates the "0" bits. The difference in transmitted probe power between these two states can be used to estimate the contribution to the extinction ratio from the saturation mechanism because there is no microwave component in the CW photocurrent to produce voltage modulation. On the other hand, the total extinction ratio can be estimated from the optical eye diagram. The contribution from photocurrent can be obtained by subtracting the contribution due to saturation from the total extinction ratio. Fig. 4 shows the results for the two terminations at different pump powers. The extinction ratios contributed by both mechanisms increase with pump power. The contribution from photocurrent with open termination is higher than that from saturation. This indicates that the photocurrent-assisted mechanism can be more effective than the saturation mechanism in a TW-EAM. The photocurrent contribution with open termination is about twice as large as that with 50-Ω termination, in close agreement with the difference in electrical eye amplitude. The operation wavelength range is also measured by changing the wavelength of the probe while adjusting the bias voltage to optimize the BER. Error-free operation is achievable over 30 nm of bandwidth with 0.5–3 dB of power penalty. The choice of the pump wavelength is not critical as the photocurrent changes by less than 15% in the entire C-band.

The fall time in the electrical eye diagram is relatively long, as shown in Fig. 2, which is due to the low reverse bias applied. A higher bias voltage is not possible for the current device because the loss will be too high for the probe. However, the optical fall time is much shorter, which can be attributed to the nonlinear transfer function of electroabsorption. The maximum speed of the current device is estimated to be 10 Gb/s, but a new material that allows higher bias has been designed to increase the speed. Also, a longer device length will lower the pump power required for a given extinction ratio, within the limits imposed by total loss and walk-off time. With the same extinction ratio, RZ format will require less pump power than the NRZ format since PAW-Conversion is peak-power dependent and RZ format has a much smaller duty-cycle. When the bit rate increases, the pump power will remain the same for NRZ format if fall time is not an issue.

IV. Conclusion

PAW-Conversion using a TW-EAM has been proposed and verified. This new design has the potential to reduce the high pumping power required by conventional approaches while adding electrical monitoring capability at the same time.

References

[1] K. Nishimura, R. Inohara, M. Tsurusawa, and M. Usami, "80 Gbit/s wavelength conversion by MQW electroabsorption modulator with delayed-interferometer," in *OFC 2003 Tech. Dig.*, vol. 1, 2003, Paper TuP5, pp. 271–273.

[2] P. S. Cho, D. Mahgerefteh, and J. Goldhar, "All-optical 2R regeneration and wavelength conversion at 20 Gb/s using an electroabsorption modulator," *IEEE Photon. Technol. Lett.*, vol. 11, pp. 1662–1664, Dec. 1999.

[3] T. Otani, T. Miyazaki, and S. Yamamoto, "40-Gb/s optical 3R regenerator using electroabsorption modulators for optical networks," *J. Lightwave Technol.*, vol. 20, pp. 195–200, Feb. 2002.

[4] E. S. Awad, P. S. Cho, C. Richardson, N. Moulton, and J. Goldhar, "Optical 3R regeneration using a single EAM for all-optical timing extraction with simultaneous reshaping and wavelength conversion," *IEEE Photon. Technol. Lett.*, vol. 14, pp. 1378–1380, Sept. 2002.

[5] H. Tanaka, T. Otani, M. Hayashi, and M. Suzuki, "Optical signal processing with electroabsorption modulators," in *OFC 2002 Tech. Dig.*, 2002, Paper WM3, pp. 262–264.

[6] S. Z. Zhang, Y.-J. Chiu, P. Abraham, and J. E. Bowers, "25 GHz polarization-insensitive electroabsorption modulators with traveling-wave electrodes," *IEEE Photon. Technol. Lett.*, vol. 11, pp. 191–193, Feb. 1999.

[7] Y.-J. Chiu, H.-F. Chou, V. Kaman, P. Abraham, and J. E. Bowers, "High extinction ration and saturation power traveling-wave electroabsorption modulator," *IEEE Photon. Technol. Lett.*, vol. 14, pp. 792–794, June 2002.

[8] H.-F. Chou, Y.-J. Chiu, and J. E. Bowers, "40 GHz optical pulse generation using sinusoidally-driven traveling-wave electroabsorption modulator," *Electron. Lett.*, vol. 38, no. 8, pp. 379–380, 2002.

[9] S. Højfeldt, F. Romstad, and J. Mørk, "Absorption recovery in strongly saturated quantum-well electroabsorption modulators," *IEEE Photon. Technol. Lett.*, vol. 15, pp. 676–678, May 2003.

[10] M. Yoneyama, Y. Miyamoto, N. Shimizu, K. Hagimoto, and T. Ishibashi, "Simple wavelength converter using an optical modulator directly driven by a uni-traveling-carrier photodiode," *Electron. Lett.*, vol. 34, no. 23, pp. 2244–2245, 1998.